ELSEVIER

Biochimica et Biophysica Acta 1236 (1995) 219–227

BBA Biochimica et Biophysica Acta

Ion channel formation by synthetic analogues of staphylococcal δ-toxin

Ian D. Kerr [a], Jean Dufourcq [b], John A. Rice [c], Donald R. Fredkin [d], Mark S.P. Sansom [a,*]

[a] *Laboratory of Molecular Biophysics, The Rex Richards Building, South Parks Road, Oxford, OX1 3QU, UK*
[b] *Centre de Récherche Paul Pascal, CNRS, Avenue A. Schweitzer, 33600 Pessac, France*
[c] *Department of Statistics, University of California, Berkeley, CA, USA*
[d] *Department of Physics, University of California at San Diego, La Jolla, CA, USA*

Received 4 October 1994; revised 17 January 1995; accepted 15 February 1995

Abstract

Ion channel formation by three analogues of staphylococcal δ-toxin, an amphipathic and α-helical channel-forming peptide, has been evaluated by measurement of ionic currents across planar lipid bilayers. Replacement of β-branched, hydrophobic residues by leucine and movement of a tryptophan residue from the hydrophilic to the hydrophobic face of the helix does not significantly alter ion channel activity. Removal of the N-terminal blocking group combined with the substitution of glycine-10 by leucine changes the single channel properties of δ-toxin, without altering macroscopic conductance/voltage behaviour. Truncation of the N-terminus by three residues results in complete loss of channel-forming activity. These changes in channel-forming properties upon altering the peptide sequence do not mirror changes in haemolytic activity. The results lend support to the proposal that channel formation and haemolysis are distinct events. Channel properties are discussed in the context of a model in which the pore is formed by a bundle of approximately parallel transbilayer helices.

Keywords: δ-Toxin; Ion channel; Amphipathic helix; Hemolysis; Channel-forming peptide

1. Introduction

δ-Toxin is a 26 residue peptide produced by the Gram positive bacterium *Staphylococcus aureus* [1]. At concentrations above ca. 2 μM δ-toxin-A (Fig. 1a) induces lysis of cells [2,3] and of synthetic phospholipid vesicles [4]. At lower concentrations (< 2 μM) δ-toxin-A forms weakly cation selective ion channels in planar lipid bilayers [5,6]. Both voltage-dependent and voltage-independent components of channel formation have been demonstrated [5]. Concentration dependence of channel formation suggests that on average each channel contains six δ-toxin-A helices [5]. This is consistent with the barrel-stave model [7,8] in which channels are formed by hexameric parallel bundles of δ-toxin-A helices packed such that the hydrophilic faces of the helices line a central aqueous pore [5,9,10]. However, whilst there are considerable data to suggest that transmembrane currents elicited by δ-toxin are due to the formation of transient ion-permeable pores [10], it has also been suggested that some amphipathic peptides may act in a detergent-like manner rather than as genuine channel-formers [11]. It therefore becomes important to distinguish between channel-formation and peptide-induced membrane lysis if the interactions between amphipathic helical peptides and lipid bilayers are to be fully understood at a molecular level.

Circular dichroism and Fourier-transform infra-red spectroscopy demonstrate a high percentage α-helical content for δ-toxin in membrane mimetic solvents [3,12–14]. NMR spectroscopic studies of δ-toxin in solution or bound to micelles support this view of the structure of δ-toxin [15–18], indicating that residues 2–20 are helical whilst the C-terminus is more disordered. Assuming that membrane bound δ-toxin-A is completely α-helical, hydrophobic moment calculations [19] suggest that it forms a highly amphipathic helix with distinct polar and apolar faces (Fig. 1b).

A number of analogues of δ-toxin-A have been synthesized in order to explore the structure–function relationships of this peptide [2,3]. Three such peptides (δ-toxins-F, -M and -L; Fig. 1) are characterized by movement of tryptophan from position 15 to position 16 and by replace-

* Corresponding author. E-mail: mark@biop.ox.ac.uk. Fax: +44 865 516454.

SSDI 0005-2736(95)00051-8

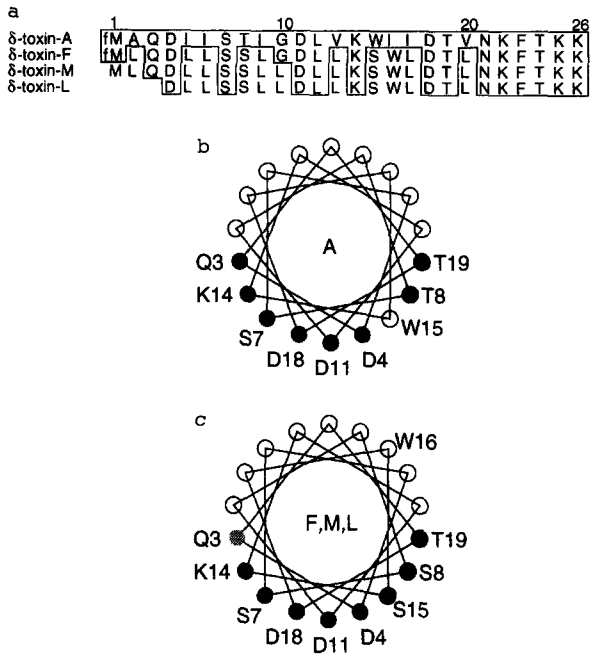

Fig. 1. δ-Toxin-A and analogues. (a) Sequences of δ-toxin peptides. Boxed regions indicate conserved residues relative to δ-toxin A. fM indicates formyl-methionine. (b,c) Helical wheel plots of δ-toxin-A (b) and δ-toxins-F, -M and -L (c). Filled circles indicate the hydrophilic face of the helix (the lighter shading of Q3 indicates its absence in δ-toxin-L). The corresponding hydrophobic moments are 0.60, 0.58, 0.58 and 0.59, respectively. The movement of tryptophan from the hydrophilic face (in δ-toxin-A) to the hydrophobic face (in δ-toxins-F, -M and -L) of the helix is indicated.

ment of β-branched hydrophobic residues by leucine. They retain the marked amphipathicity of the native δ-toxin-A. δ-Toxins-M and -L also possess a net positive charge as a result of loss of the formyl blocking group from the N-terminus. In addition, δ-toxins-M and -L differ from δ-toxins-A and -F in that glycine-10 is replaced by leucine. Furthermore, δ-toxin-L is three residues shorter at the N-terminus than the other peptides.

All three δ-toxin analogues retain the membrane lytic activity of δ-toxin A [2,20], and all are α-helical in lipid micelles (Table 1). Fluorescence intensity measurements on δ-toxins-A and -F [3] are consistent with the hypothesis that, in the absence of a transbilayer potential, δ-toxin binds to membranes with the hydrophilic face of the helix oriented towards the aqueous solution, and the hydrophobic face exposed to the lipid tails.

Here we describe the channel-forming properties of δ-toxin-F, -M and -L. Comparisons are made with channels formed by δ-toxin-A [5,6]. The results are correlated with the known secondary structure and haemolytic activity of the peptides in order to determine possible structure–function relationships.

Table 1
Comparison of channel and haemolytic properties of δ-toxin analogues

Property	δ-Toxin analogue			
	A	F	M	L
Conductances (pS)	30	60	36	–
	80–100	100–200		
	ca. 450	> 200		
Haemolytic activity [a]	100	25	30	67
% Helicity [b]	75±5	68±5	70±5	72±5

[a] Haemolytic activities are relative to that of the natural toxin (A) and measured at 2.5 μM [2,20].

[b] % helicity determined by CD spectroscopy in the presence of lyso-phosphatidylcholine micelles [3] or when bound to phosphatidylcholine/phosphatidylserine micelles [20].

2. Materials and methods

δ-Toxin analogues F, M and L were synthesized and purified as described previously [2,3]. Stock solutions of δ-toxins were dissolved in 1% TFA (pH 2.1) and stored at −80° C until required. Toxin concentrations were estimated using the molar absorption coefficient of tryptophan at 280 nm ($\epsilon = 5500\ M^{-1}\ cm^{-1}$).

Planar lipid bilayers were formed as described by Montal and Mueller [21]. Briefly, the bilayer is formed across a small (ca. 100 μm diameter) circular or elliptical aperture in a thin (25 μm) piece of Teflon film (Yellow Springs Instruments, OH) by the apposition of two lipid monolayers spread at an air/water interface on either side of a Teflon septum. After formation of a stable bilayer, peptide solutions were added, with stirring, to one face of the bilayer to a final concentration in the range 0.2 to 2.0 μM. Channel formation, when present, was usually observed within 15 min of toxin addition. The buffer used was 0.5 M KCl, 10 mM Bes, pH 7.0, unless otherwise stated. In all experiments the lipid used was 1,2-diphytanoylphosphatidylcholine [22] (Avanti Polar Lipids, AL).

The following convention is adopted with respect to the sign of the transmembrane potential. The chamber to which peptide is added is referred to as the *cis* chamber, and all electrical potential measurements refer to this side. The other (*trans* chamber) is electrically grounded through the head-stage. Transbilayer electrical currents were measured with an Axopatch 1D amplifier (Axon Instruments, CA) and recorded on a Betamax video recorder, after processing by a pulse-code modulator (sampling rate 44.1 kHz). Data for analysis was filtered by an 8-pole low-pass Bessel filter. Data acquisition was performed using the ASYST software package (ASYST Software Technologies, Rochester, NY), running on a 286 processor based PC fitted with a DAS-16 A/D converter (Keithley Instruments, Reading).

Persistence function analysis was carried out as described elsewhere [23,24]. Briefly, the persistence function $\phi(I,t)$ gives the probability density for observing a current, I, at time, t, conditional on having observed the same current at time $t = 0$, i.e.:

$$\phi(I,t) = f(I_t|I_0)$$

Thus, if a current level corresponds to a true conducting state the persistence function should be high and decay relatively slowly with increasing t. Electrical noise, however, should rapidly decay with t [23,24].

3. Results

3.1. Channel formation by δ-toxins-F, -M and -L

Planar lipid bilayer experiments were conducted at peptide concentrations between 0.2 and 2.0 μM, and transbilayer potentials between −200 and +200 mV. Of 96 experiments on δ-toxin-F, 69 yielded discrete channel activity, and of 35 experiments on δ-toxin-M, 27 yielded channel formation. This frequency of channel formation is comparable to that observed for δ-toxin-A [5]. However, in all 12 experiments on δ-toxin-L no channel formation was ever observed (Table 1). No evidence of channel formation was observed for δ-toxin-L, even at concentrations of 2 μM when applying a range of membrane potentials from −200 mV to +200 mV. In contrast, channel formation by the other two analogues was observed at from ca. 0.5 to 1 μM peptide. Electrical breakdown of the lipid bilayer occurred at δ-toxin-F concentrations greater than ca. 2 μM.

3.2. δ-Toxin-F single channel properties

Fig. 2a shows the entire 300 s duration of a single channel recording made using 0.7 μM δ-toxin-F at −160 mV. There are clear transitions between open and closed states, with the channel predominantly in an open state for much of the recording. The δ-toxin-F channel exhibits two

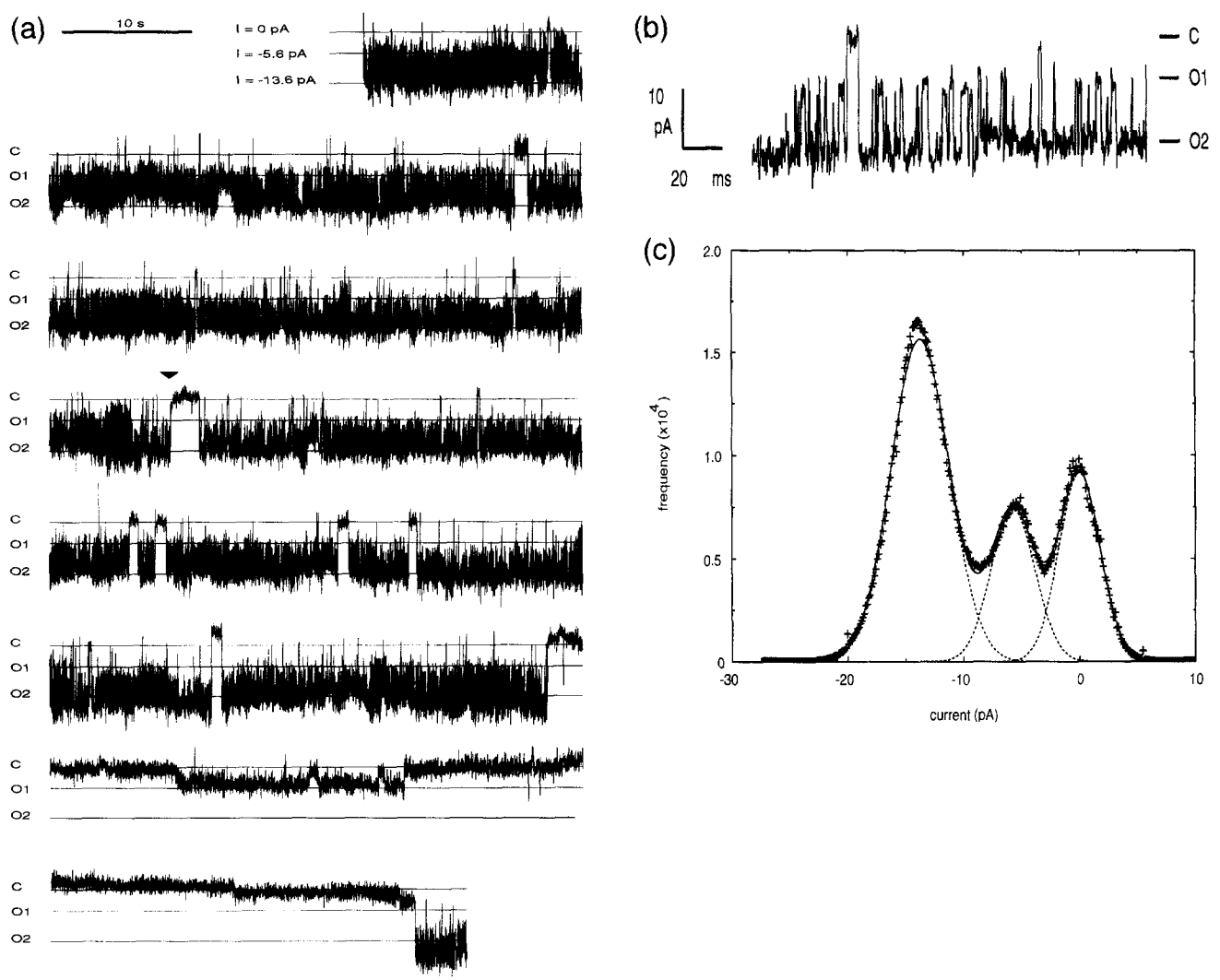

Fig. 2. Channel formation by δ-toxin-F. (a) The entire data stretch, duration 300 s. Three states are indicated (C, O1 and O2) as determined from the current amplitude histogram of the data (Fig. 2c). The data have been resampled at 100 Hz, leading to rounding off of transitions between open and closed states (for example, indicated by an arrow in the fourth trace). (b) A small segment of the recording in (a) shown on a faster time scale to resolve individual channel events. Transitions are visible between C and O2, and O1 and O2. (c) Current amplitude histogram for the entire data stretch in (a). Crosses represent the data, which can be fitted as the sum of three Gaussian distributions (solid line). Dotted lines represent the individual Gaussian components which give the probability and current of the three states (see text). Histogram was calculated on data sampled at 5 kHz and filtered at 2 kHz.

modal open states with a spectrum of conductance levels centred about these. Channel open times are in the millisecond range. The closed state, C, and two modal open states, O1 and O2, are visible. On detailed inspection (Fig. 2) transitions are observed between C and O1, O1 and O2, and between C and O2. This suggests that conductance fluctuations may be due to alternative conformations of the same channel. Fig. 2c represents the current amplitude histogram of the entire data stretch of Fig. 2a. The fitted conductances, G_j, and probabilities, P_j, of the three states are: $G_0 = 0$ pS (closed), $P_0 = 0.24$; $G_1 = 35$ pS (O1), $P_1 = 0.20$; $G_2 = 88$ pS (O2), $P_2 = 0.56$. Hence, the channel is open in one or other open state for 76% of the time. These properties are similar to those observed for δ-toxin-A [5,6].

δ-Toxin-F channels have been recorded using 0.2, 0.5, 1.0, and 3.0 M KCl. Overall, a decrease in $< P_C >$ (the mean probability of the closed state) is observed from 0.56 (S.D. = 0.28, $n = 8$) at 0.5 M KCl, to 0.36 (S.D. = 0.21, $n = 6$) at 3.0 M KCl. These data provide evidence for stabilization of open states at higher KCl concentrations. This has been reported for a number of other channel-forming peptides and may reflect decreased helix-helix repulsion as a result of increased electrostatic screening by electrolyte both within and at the mouths of the channels [5,25,26].

Single channel conductances in electrolyte concentrations other than 0.5 M have been normalized using the equivalent conductivities of salt solutions. A broad range of open channel conductances is observed from 4 pS to ca. 0.7 nS. However, some degree of clustering of conductance states is apparent, with 'low' conductance states (< 60 ps), 'medium' conductance states (80–200 pS), and 'high' conductance states (> 200 pS). Such clustering of conductance states is similar to that previously observed for δ-toxin-A [5,6].

The relative brevity of the single channel openings induced by δ-toxin-F raises the possibility that analysis of conductance levels using current amplitude histograms may overlook 'hidden' conductance levels. Persistence function analysis [23,24] enables identification of conductances obscured in amplitude histograms. Fig. 3 represents the persistence function for the entire data set in Fig. 2a. The current division is 0.25 pA and t ranges from 0 to 1.0 s. The function identifies four conductance states which decay slowly with time. The conductances of the four states are −7 pS, +6 pS, +28 pS and +89 pS. The first two levels both represent the closed channel. Splitting of the closed channel level between −7 and +6 pS reflects the small degree of baseline shift, which can be seen at the end of the recording in Fig. 2a. The two open channel levels (+28 and +89 pS) are equivalent to O1 and O2 as observed in current amplitude histogram analysis above. Thus, in this case there is no evidence for the presence of additional hidden conductance levels.

3.3. Voltage gating of δ-toxin-F channels

The relationship between δ-toxin-F channel formation and transbilayer potential may be explored by determina-

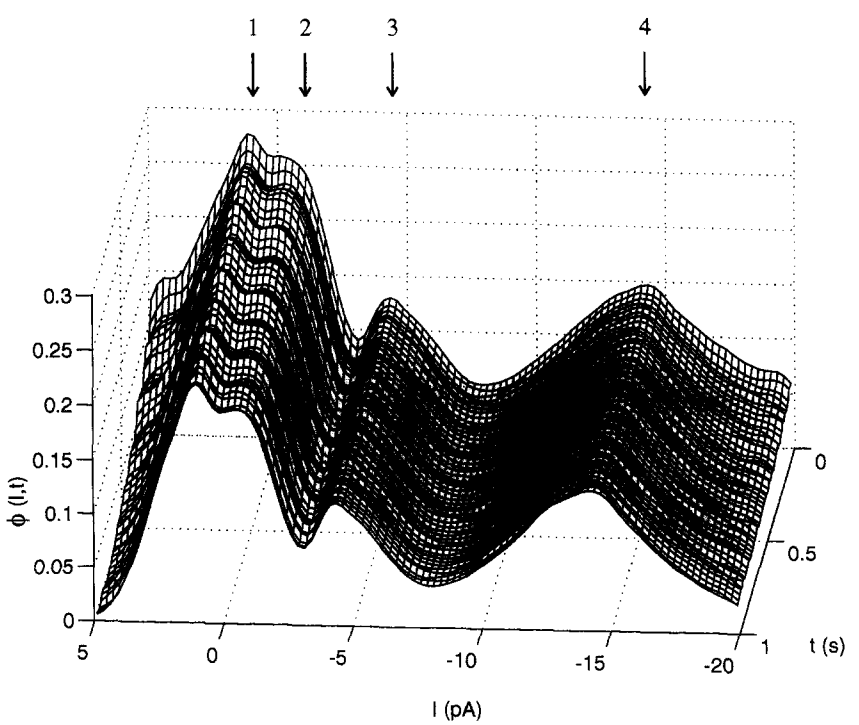

Fig. 3. Persistence function analysis of δ-toxin-F. Persistence, $\phi(I,t)$, of ionic current for the entire data set in Fig. 2a with a current division of 0.25 pA and t from 0 to 1.0 s (see text). The four peaks in the persistence function are labelled 1, 2, 3 and 4.

tion of macroscopic current/voltage (I/V) curves. Such data provide insights into possible mechanisms of channel formation. I/V curves were determined by the application of a slow (typically 20 s peak-to-peak) triangular wave of membrane potential, to bilayers for which channel activity had already been observed at constant potentials.

Results of such an experiment, with a wave duration of 25 s and a magnitude of ±160 mV, are shown in Fig. 4. It can be seen that channel formation occurs at both positive and negative potentials, although somewhat more readily at the former. The magnitude of the current measured at the voltage extremes (from left to right: ca. 90 pA, 160 pA and 65 pA) indicates the formation of multiple channels (between 4 and 10 per wave) rather than high conductance single channels. This is confirmed by short time-scale inspection of individual waves which revealed multiple channel events at the voltage extremes.

Current/voltage curves are derived by summing such I/V data. The result of summing 50 consecutive membrane potential waves from the same bilayer is shown in Fig. 4b. There are several features of the summed I/V curve that merit mention. Firstly, the curve shows both a linear, voltage-independent section (between approx. ±80 mV) and a very noticeable non-linear section at higher potentials. The presence of non-linearity in the average I/V curve is an indicator of a voltage-dependent component to channel formation. Non-linearity of I/V curves has been demonstrated for δ-toxin-A [5], and other channel-forming peptides [27,28]. The evident non-linear conductance in the average I/V curve suggests that channel formation by δ-toxin-F is predominantly voltage-dependent. Additionally, though channel formation occurs at both positive and negative potentials, there is evidence that channels are more favoured at *cis* positive potentials. Thus, to achieve a total current of 500 pA a potential of *cis* +115 mV is required, compared with a potential of −154 mV to achieve the same total current (Fig. 4b).

3.4. Ionic selectivity of δ-toxin-F channels

The cation/anion selectivity of δ-toxin-F channels was determined by measuring the reversal potential (V_{rev}) in the presence of asymmetric KCl concentrations across the bilayer. A macroscopic I/V relationship derived by summing 20 waves (magnitude ±120 mV, duration 20 s] with $[KCl]_{cis} = 0.2$ M and $[KCl]_{trans} = 1.0$ M yielded a reversal potential of ca. +15 mV. Substitution of these values in the Goldman-Hodgkin-Katz equation [29]:

$$\frac{P_K}{P_{Cl}} = \frac{\alpha[KCl]_{trans} - [KCl]_{cis}}{[KCl]_{trans} - \alpha[KCl]_{cis}}$$

where:

$$\alpha = \exp\frac{(FV_{rev})}{RT}$$

gives $P_K/P_{Cl} = 2.5$, i.e., the channels formed by δ-toxin-F are 2.5-times more permeable to potassium ions than chloride ions.

Because of the voltage-dependence of channel activation it proved difficult to determine an exact value of V_{rev} by single channel measurements, but lower and upper limits of the reversal potential of +5 and +15 mV (giving a selectivity of between 1.3 and 2.5) were obtained, in agreement with the estimate obtained from analysis of macroscopic I/V data. The agreement between the two methods for the determination of ionic selectivity suggests that the voltage-dependent and voltage-independent conductances correspond to the same channel.

3.5. δ-Toxin-M single channel properties

Fig. 5a shows the entire 420 s duration of a typical recording made using 0.8 μM δ-toxin-M, at a membrane potential of −120 mV (i.e., similar conditions to those employed for δ-toxin-F in Fig. 2a). Channel activity is absent from long stretches of the recording, with a long

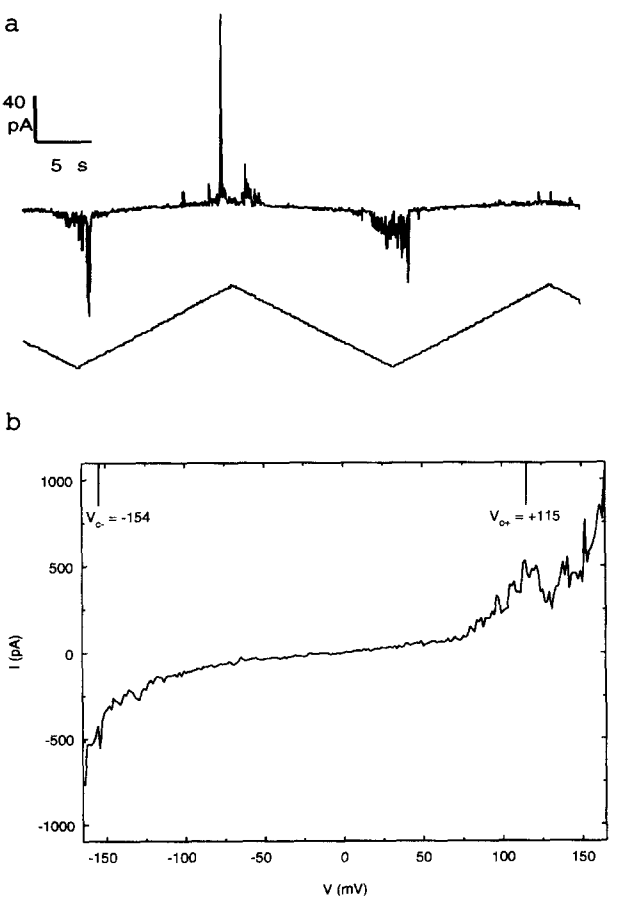

Fig. 4. Current/voltage relationship of δ-toxin-F. (a) Representative segment of the current measured (upper trace) in response to a triangular potential wave of ±160 mV (lower trace). (b) The total current/voltage curve obtained by summing 50 such waves. Vertical, solid lines indicate the potential (V_c) required to exceed a current magnitude of 500 pA (see text). Data were filtered at 500 Hz and sampled at 83 Hz.

(50 s) burst of activity in the middle of the recording and a shorter activation at the start. Occasional, briefer bursts are seen at other points.

Detailed inspection of the recording suggests that multiple conductance levels are present, but if a stretch of these data are redisplayed on a shorter time scale (Fig. 5b), single channel events can barely be resolved. The channel switches rapidly from a closed state (C) to one or more open states. This is reflected in the current amplitude histogram (Fig. 5c) which corresponds to a broad envelope of conductance levels from ca. 40 pS to ca. 160 pS. Increasing the KCl concentration from 0.5 M to 3.0 M did not result in discrete, resolved channel openings.

In an attempt to resolve possible 'hidden' single channel conductance states from within the spread of observed conductances, persistence function analysis was carried out for the entire stretch of data shown in Fig. 5a. Such analysis has been demonstrated to be capable of picking out conductance levels not apparent from current amplitude histograms when tested using physiological channel data (Rice, unpublished observations). As for δ-toxin-F, t ranges from 0 to 1.0 s, while the current division is 0.33 pA. The results of the analysis are shown in Fig. 6. Two states are resolved by the function: the closed state (marked C) with a current 0 pA ($G = 0$ pS) and an open state (marked O1) with a single-channel current of −4.3 pA ($G = 36$ pS). The open state identified corresponds to the location of the shoulder in the current amplitude histogram (Fig. 5c) and is comparable to the lowest conductance state observed for both δ-toxins-A and -F [6] (see above).

3.6. Voltage gating of δ-toxin M

Fig. 7a displays a sample stretch of data from a current-voltage experiment, with a wave duration of 15 s and magnitude of ± 120 mV. As was observed for δ-toxin-F there is channel activity at both positive and negative potentials. The currents at the extreme potentials indicate

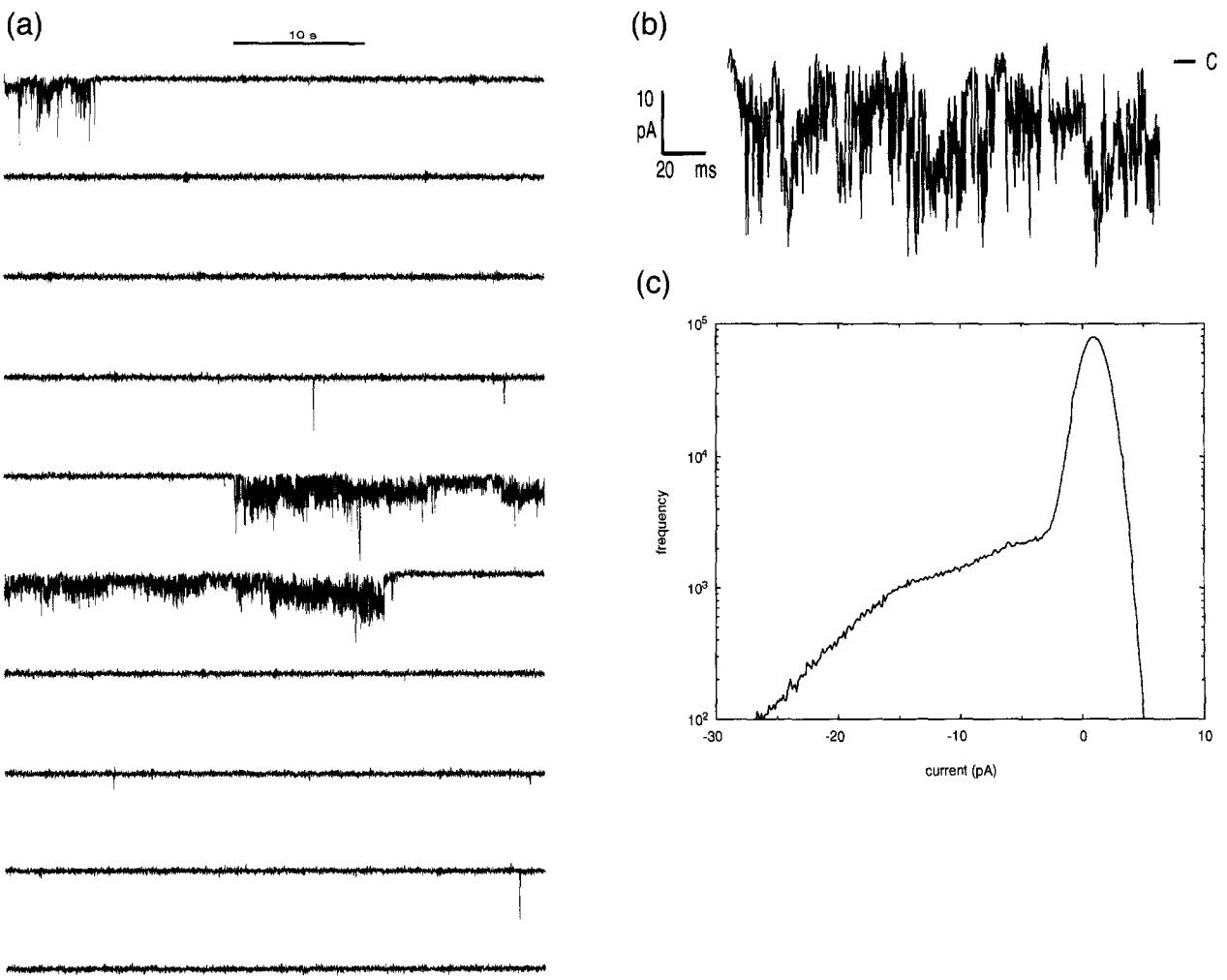

Fig. 5. Ion channel formation by δ-toxin-M. (a) The entire 420 s data stretch. Channel openings are downward deflections from the closed state C. The recording is mainly in the closed state with a long activation in the middle and a shorter one at the start. The data have been resampled at 100 Hz. (b) A section of the recording from the long active segment shown on an expanded time scale. The closed state is denoted by C. (c) Corresponding current amplitude histogram on a logarithmic scale for the entire data stretch in (a).

the presence of multiple channels (assuming a single channel conductance of ca. 30 to 40 pS). The summed I/V curve is shown in Fig. 7b. The resemblance to that determined for δ-toxin-F is clear. There is again evidence that channel formation is more pronounced at *cis* positive than *cis* negative potentials. The lower total current for δ-toxin M compared to δ-toxin-F is due to more inactive waves in the δ-toxin-M experiment. δ-Toxin-M also shows a voltage-independent conductance between ca. ±70 mV, with non-linear current/voltage behaviour at greater potentials. An estimate of the single channel conductance of δ-toxin-M (obtained from analysis of the slope of the voltage-independent sections of individual current/voltage waves) reveals a mean slope conductance of the order of 45 pS (±15 pS), comparable to the single channel conductance level identified in persistence function analysis.

4. Discussion

Three synthetic analogues of δ-toxin-A have been investigated for their ability to form channels in planar bilayers. The results demonstrate that replacement of hydrophobic β-branched residues by leucine does not significantly affect channel formation. However, the removal of three N-terminal residues results in the abolition of channel-formation. It must be emphasised that the ability of the peptides to form channels does not correlate with their ability to induce haemolysis. The three analogues studied here have lower haemolytic activity than δ-toxin-A (Table 1). δ-Toxin-F and δ-toxin-M are 3- to 4-times less active than δ-toxin-A, yet display comparable channel-forming activity [3]. Conversely, truncating the N-terminus of δ-toxin-M (to give δ-toxin-L) enhances the lytic activity 2- to 3-fold, while abolishing channel formation [20] (Table 1). This difference between channel-forming and lytic activities is of considerable importance as it contradicts the view that channel formation by amphipathic, helical peptides is a non-specific, detergent-like action. That is, our results demonstrate that channel formation is not simply due to limited membrane lysis. Instead it appears that channel formation and haemolysis by δ-toxin are distinct events, which occur in parallel rather than sequentially, with channel formation occurring at lower δ-toxin concentrations than does haemolysis. Such a distinction between channel formation and haemolysis has also been made for melittin on the basis of studies employing synthetic analogues [30].

4.1. Comparison of channel formation by δ-toxin-A and -F

The channel-forming properties of δ-toxin-A and δ-toxin-F are quite similar. This suggests that the structures of the channels formed by the two toxins must be similar. Both toxins exhibit channel formation at sub-micromolar concentrations, with electrical breakdown of membranes at concentrations higher than 2 μM. The single channel conductances of δ-toxins-A and -F are also very similar, and both display weak cationic selectivity. Both toxins exhibit clusters of 'low' (ca. 30 pS), 'medium' (ca. 100

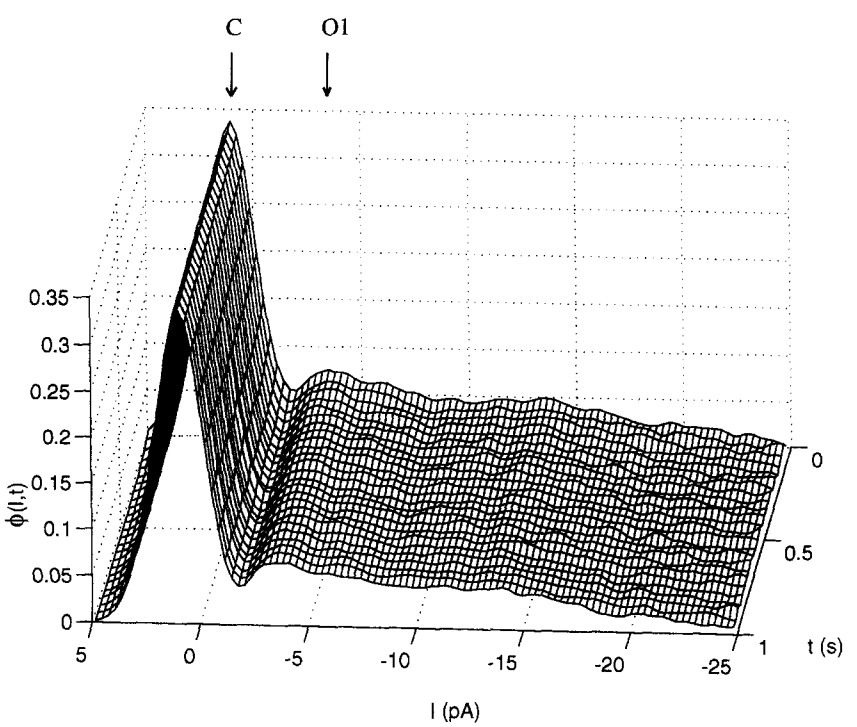

Fig. 6. Persistence function analysis of δ-toxin-M. Persistence function analysis of the entire data set in Fig. 5a with a current division of 0.33 pA and t from 0 to 1.0 s. The two peaks in the persistence function are labelled C and O1, corresponding to the closed and open channel conductance levels.

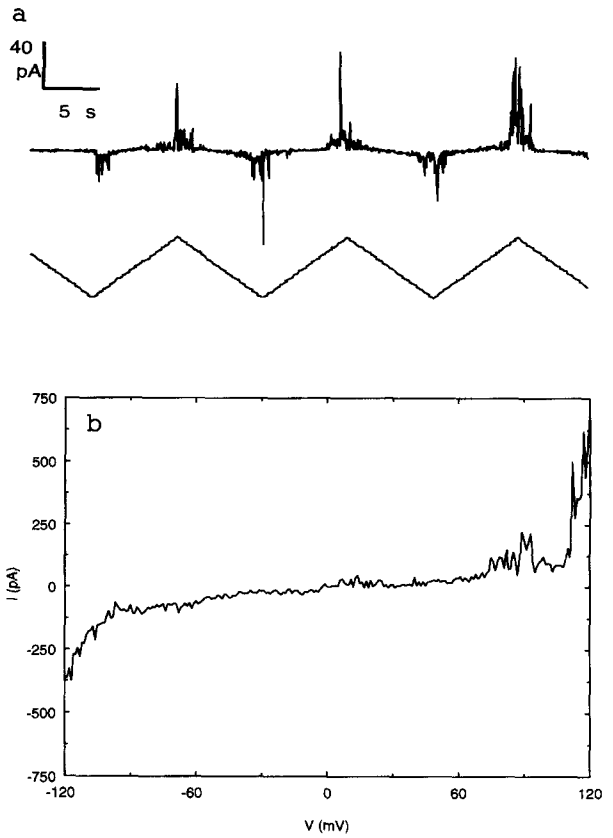

Fig. 7. Current/voltage relationship of δ-toxin-M as measured by the response to a slow transbilayer potential wave of ±120 mV. (a) Individual waves displaying macroscopic ion channel formation (upper trace) at both positive and negative potentials (lower trace). (b) The overall current/voltage curve of 50 such waves. Voltage dependent channel openings occur at potentials greater than ±70 mV. Data were filtered at 500 Hz and sampled at 83 Hz.

pS) and 'high' (several hundred pS) conductance states. Furthermore, both δ-toxin-A and -F have open channel lifetimes of the order of 1 ms. Preliminary modelling studies of δ-toxin-A channels suggested that conformational changes in the sidechain of the tryptophan residue at position 15 might be responsible for the flickering of channel conductances between substates [31]. However, the persistence of rapid transitions between conductance substates in δ-toxin-F demonstrates that such gating is not mediated by conformational changes in tryptophan sidechains, and requires more detailed modelling to explain rapid flickering.

Our results provide evidence that the channels formed by δ-toxin-F are composed of approximately parallel (rather than anti-parallel) helical aggregates. Firstly, channels are observed when δ-toxin-F is added to only one side of the bilayer. Although some degree of voltage-dependent 'flip-flop' of peptide within the bilayer cannot be completely excluded we feel this is unlikely to occur with highly ordered lipid chains such as those of diphytanoylphosphatidylcholine. Secondly, channels are stabilized by high electrolyte concentrations, consistent with screening of the repulsive electrostatic interactions which would be present within a parallel bundle of helices. This is supported by molecular modelling studies which indicate a role for electrolyte screening of the partial charges of residues glutamine-3, aspartate-4, lysine-25 and lysine-26 at the termini of δ-toxin-F in parallel aggregates. Thirdly, the moderately voltage-dependent channel gating and the asymmetry (albeit limited) of macroscopic current/voltage curves support a parallel helix model for channel formation by δ-toxin-F, with a transmembrane potential required to overcome the repulsion due to parallel aligned helix dipoles. Thus, the experimental results appear to be inconsistent with the model of Raghunathan et al. [32] in which adjacent helices are antiparallel. Models of δ-toxin-F channels based on parallel helix bundles have been generated by restrained molecular dynamics simulations, and will form the subject of a subsequent publication (Kerr and Sansom, unpublished data).

4.2. δ-Toxins-M and -L

Although the macroscopic current/voltage properties of δ-toxin-M are similar to those of δ-toxin-F, it fails to form discrete and stable single channels. In parallel transmembrane bundles the juxtaposition of free N-termini of adjacent N-termini (as opposed to the formylated N-termini of δ-toxin-F) would generate an additional electrostatic destabilization, which may explain the very brief channel lifetimes. A correlation may be drawn with a de novo designed leucine- and serine-containing channel-forming peptide [33] for which neutralization of a free N-terminus by acetylation resulted in stabilization of the channel open state [34].

Truncation of the first three residues of δ-toxin-M, to yield δ-toxin-L, results in complete loss of channel formation. δ-Toxin-M and -L have similar secondary structures, as determined by CD spectroscopy [2,3,20], and so one might anticipate that δ-toxin-L should be able to form bundles of transbilayer helices. However, attempting to form such a bundle of the truncated peptide spanning an undistorted bilayer would result in the highly charged C-termini of the helices being drawn into the low-dielectric environment of the lipid bilayer. This would be energetically unfavourable, and so could prevent channel formation. However, one should note that truncation of the N-terminus also removes residue glutamine-3 from δ-toxin-L. Molecular modelling studies indicate that rings of glutamine residues contribute towards stabilization of helix bundles formed by δ-toxins-A and -F (Kerr and Sansom, unpublished data). It is therefore possible that residue glutamine-3 stabilises δ-toxin -A, -F and -M helix bundles, whereas such inter-helix interactions are not possible for δ-toxin-L. It should be noted that a ring of glutamine residues has also been implicated in helix bundle stabilization for the channel-forming peptide alamethicin [35,36].

Overall, the altered channel-forming properties of δ-toxin-M and -L relative to δ-toxin-F may be rationalized in terms of a channel model based on a parallel helix bundle, in agreement with the barrel-stave model proposed for alamethicin [7,8], thus providing support for the applicability of this mechanism to a wider range of channel-forming peptides.

Acknowledgements

This work was supported by a grant from the Wellcome Trust and by an SERC/CASE studentship with Shell Research Ltd. Dr. O. Siffert (Unité de Chimie Organique, Institut Pasteur, Paris) and Dr. E. Thiaudière (Institut de Biochimie de Génétique Cellulaire, Université de Bordeaux II) are acknowledged for synthesis of the peptides.

References

[1] Fitton, J.E., Dell, A. and Shaw, W.V. (1980) FEBS Lett. 115, 209–212.
[2] Alouf, J.E., Dufourcq, J., Siffert, O., Thiaudière, E. and Geoffroy, C. (1989) Eur. J. Biochem. 183, 381–390.
[3] Thiaudière, E., Siffert, O., Talbot, J.C., Bolard, J., Alouf, J.E. and Dufourcq, J. (1991) Eur. J. Biochem. 195, 203–213.
[4] Yianni, Y.P., Fitton, J.E. and Morgan, C.G. (1986) Biochim. Biophys. Acta 856, 91–100.
[5] Mellor, I.R., Thomas, D.H. and Sansom, M.S.P. (1988) Biochim. Biophys. Acta 942, 280–294.
[6] Sansom, M.S.P. and Mellor, I.R. (1988) in Neurotox '88: Molecular basis of drug and pesticide action (Lunt, G.G., ed.), pp. 419–428, Elsevier, Amsterdam.
[7] Boheim, G. (1974) J. Membr. Biol. 19, 277–303.
[8] Baumann, G. and Mueller, P. (1974) J. Supramol. Struct. 2, 538–557.
[9] Freer, J.H. and Birkbeck, T.H. (1982) J. Theor. Biol. 94, 535–540.
[10] Sansom, M.S.P. (1991) Progr. Biophys. Mol. Biol. 55, 139–236.
[11] Saberwal, G. and Nagaraj, R. (1994) Biochim. Biophys. Acta 1197, 109–131.
[12] Colacicco, G., Basu, M.K., Buckelew, A.R. and Bernheimer, A.W. (1977) Biochim. Biophys. Acta 465, 378–390.
[13] Fitton, J.E. (1981) FEBS Lett. 130, 257–260.
[14] Brauner, J.W., Mendelsohn, R. and Prendergast, F.G. (1987) Biochemistry 26, 8151–8158.
[15] Lee, K.H., Fitton, J.E. and Wüthrich, K. (1987) Biochim. Biophys. Acta 911, 144–153.
[16] Tappin, M.J., Pastore, A., Norton, R.S., Freer, J.H. and Campbell, I.D. (1988) Biochemistry 27, 1643–1647.
[17] Bladon, C.M., Bladon, P. and Parkinson, J.A. (1992) Biochem. Soc. Trans. 20, 862–864.
[18] Bladon, C.M., Bladon, P. and Parkinson, J.A. (1993) J. Chem. Soc. Perkin Trans. I. 109, 1687–1697.
[19] Eisenberg, D., Weiss, R.M. and Terwilliger, T.C. (1982) Nature 299, 371–374.
[20] Cornut, I. (1993) PhD Thesis, Université de Bordeaux I, Bordeaux.
[21] Montal, M. and Mueller, P. (1972) Proc. Natl. Acad. Sci. USA 69, 3561–3566.
[22] Redwood, W.R., Pfeiffer, F.R., Weisbach, J.A. and Thompson, T.E. (1971) Biochim. Biophys. Acta 233, 1–6.
[23] Fredkin, D.R. and Rice, J.A. (1993) Technical Report 391, University of Berkeley, Statistical Department, Brekeley.
[24] Fredkin, D.R. and Rice, J.A. (1994) Biophys. J. 66, A354.
[25] Hanke, W., Methfesell, C., Wilmsem, H-U., Katz, E., Jung, G. and Boheim, G. (1983) Biochim. Biophys. Acta 727, 108–114.
[26] Woolley, G.A., Epand, R.M., Kerr, I.D., Sansom, M.S.P. and Wallace, B.A. (1994) Biochemistry 33, 6850–6858.
[27] Hall, J.E., Vodyanoy, I., Balasubramanian, T.M. and Marshall, G.R. (1984) Biophys. J. 45, 233–247.
[28] Tosteson, M.T. and Tosteson, D.C. (1981) Biophys. J. 36, 109–116.
[29] Hille, B. (1992) Ionic Channels of Excitable Membranes, pp. 347–353, Sinauer, MA.
[30] Dempsey, C.E., Bazzo, R., Harvey, T.S., Syperek, I., Boheim, G. and Campbell, I.D. (1991) FEBS Lett. 281, 240–244.
[31] Sansom, M.S.P., Kerr, I.D. and Mellor, I.R. (1991) Eur. Biophys. J. 20, 229–240.
[32] Raghunathan, G., Seetharamulu, P., Brooks, B.R. and Guy, H.R. (1990) Prot. Struct. Funct. Genet. 8, 213–225.
[33] Lear, J.D., Wasserman, Z.R. and and DeGrado, W.F. (1988) Science 240, 1177–1181.
[34] Åkerfeldt, K.S., Lear, J.D., Wasserman, Z.R., Chung, L.A. and DeGrado, W.F. (1993) Acc. Chem. Res. 26, 191–197.
[35] Fox, R.O. and Richards, F.M. (1982) Nature 300, 325–330.
[36] Sansom, M.S.P. (1993) Q. Rev. Biophys. 26, 365–421.